

1 On the Effect of Model Parameters on Forecast Objects

2 Caren Marzban^{1,2*}, Corinne Jones², Ning Li², Scott Sandgathe¹

¹ Applied Physics Laboratory

² Department of Statistics

Univ. of Washington, Seattle, WA 98195 USA

3 ABSTRACT

4 Many physics-based numerical models produce a gridded, spatial field of forecasts, e.g., a
5 temperature “map.” The field for some quantities generally consists of spatially coherent
6 and disconnected “objects.” Such objects arise in many problems, including precipitation
7 forecasts in atmospheric models, Eddy currents in ocean models, and models of forest fires.
8 Certain features of these objects (e.g., location, size, intensity, and shape) are generally of
9 interest. Here, a methodology is developed for assessing the impact of model parameters
10 on features of forecast objects. The main ingredients of the methodology include the use of
11 1) Latin hypercube sampling for varying the values of the model parameters, 2) statistical
12 clustering algorithms for identifying objects, 3) multivariate multiple regression for assessing
13 the impact of multiple model parameters on the distribution (across the forecast domain) of

*Corresponding Author: marzban@stat.washington.edu

14 object features, and 4) methods for reducing the number of hypothesis tests, and controlling
15 the resulting errors. The final “output” of the methodology is a series of boxplots and
16 confidence intervals that visually display the sensitivities. The methodology is demonstrated
17 on precipitation forecasts from a mesoscale numerical weather prediction model.

18 The author’s copyright for this publication is transferred to University of Washington.

1. Introduction

Complex, physics-based numerical models of natural phenomena often have parameters - henceforth, model parameters - whose values are generally not *a priori* specified. In such situations it is important to infer the manner in which the model parameters affect the outputs of the model (i.e., forecasts, or predictions), and often the techniques of Sensitivity Analysis (SA) are employed to assess the effects. There is a wide range of techniques from relatively simple one-at-a-time method (also known as the Morris method) where each model parameter is varied individually (e.g., Yu et al. (2013)), to multivariate approaches motivated by statistical methods of experimental design (Montgomery 2009) where the values of the model parameters are varied according to some optimization criterion. Alternative approaches can be found in Backman et al. (2017) where algorithmic differentiation is used, and in Kalra et al. (2017) where the underlying physics equations are integrated using quadrature methods. And yet another alternative is the adjoint method, commonly used in meteorological circles (Errico 1997).

It is difficult to classify the various methods into a simple taxonomy (Bolado-Lavin and Badea 2008), but the terms Local and Global have been used to denote two broad categories (Saltelli et al. 2010, 2008); generally, local methods employ some sort of derivative of the model output with respect to inputs, while global techniques rely on a decomposition of the variance of the output in terms of the variance explained by the inputs. Comparisons of the various approaches are not common-place, because each approach is usually suited for a specific application where other methods may not be practically feasible. However, an example of the comparison of one global approach and one local (adjoint) approach on the

41 Lorenz '63 model (Lorenz 1963) has been performed by Marzban (2013).

42 Another possible classification criterion is based on the purpose of the SA. Some SA
43 work is performed for assessing how model parameters impact the model itself, not as a
44 means to some other goal. For example, Lucas et al. (2013) uses a global SA method to
45 explore the effect of model parameters on the probability of model crashes. By contrast,
46 sometimes SA is performed as an intermediate step to another goal, such as the calibration
47 of the model (Safta et al. 2015; Hacker et al. 2011; Laine et al. 2012; Ollinaho et al. 2014).
48 All of these classification criteria are imperfect, as there exist works which fall “between”
49 Global versus Local, or SA-only versus SA-for-calibration; some examples include Roebber
50 (1989); Roebber and Bosart (1989); Robock et al. (2003). The work reported here falls into
51 the Local and SA-only category; as such, although the proposed methodology can be used
52 for calibration, no attempt is made to do so here.

53 In many SA studies, the output of the model (i.e., the response variable in the SA) is
54 usually a single or a handful of scalar quantities. But there are situations in which the output
55 is a gridded spatial field, e.g., temperature forecasts over a spatial region. Every grid point
56 reflects a forecast at that location, and for a quantity like temperature the field as a whole
57 has a smooth, continuous nature. SA is more complicated for precipitation fields, where
58 the model output is a quantity whose spatial structure is not smooth and/or continuous.
59 Indeed, there may be a coherent set of grid points that receive no precipitation at all, while
60 an adjacent set of grid points will reflect a complex pattern of precipitation. In short, the
61 spatial field of such quantities will contain “objects” within which precipitation does occur,
62 surrounded by regions of little or no precipitation. Such objects arise in a wide range of
63 Earth systems, e.g., models of ocean currents and eddies (e.g., Fig. 1 in Samsel et al.

64 (2015)), atmospheric plume/dispersion (e.g., Fig. 4 in Stein et al. (2015)), ocean garbage
65 transport (e.g., Fig. 2 in Froyland et al. (2014)), forest fires (e.g., Fig. 8 in Vogelmann et al.
66 (2011)), and models of the Earth’s mantle (e.g., Fig. 4. in French et al. (2013)).

67 For such discrete fields, the assessment of the quality of the forecasts has given rise to a
68 wide range of specialized techniques generally referred to as spatial verification (or evalua-
69 tion) (Ahijevych et al. 2009; Baldwin et al. 2001, 2002; Brown et al. 2002; Casati et al. 2004;
70 Davis et al. 2006a,b; Du and Mullen 2000; Ebert 2008; Ebert and McBride 2000; Gilleland
71 et al. 2009; Hoffman et al. 1995; Keil and Craig 2007; Marzban and Sandgathe 2006, 2008;
72 Marzban et al. 2008, 2009; Nachamkin 2004; Roberts and Lean 2008; Wealands et al. 2005;
73 Wernli et al. 2008; Venugopal et al. 2005; Li et al. 2015). A subset of these methods employs
74 the notion of an object explicitly. In some applications, the object is defined subjectively
75 - for example, by human experts. In other applications statistical methods for clustering
76 (Everitt 1980) are used to identify/define objects within the field (Marzban and Sandgathe
77 2006, 2008). This clustering approach, which has been re-examined by Lakshmanan and
78 Kain (2010), and more recently by Wang et al. (2015), is the basis of the object-identification
79 procedure used in the present work.

80 Although no spatial verification/evaluation is done here, the importance of objects within
81 the forecast field calls for a SA framework wherein one can assess the effect of model param-
82 eters on features of the objects. Also, the assessment of sensitivity is highly intertwined with
83 that of statistical significance. The methodology developed here can be viewed as an object-
84 based SA with which one can assess the impact (both the magnitude and the statistical
85 significance) of model parameters on object features.

86 More specifically, the next section describes the main components of the proposed

87 methodology, namely Latin hypercube sampling for determining how the model parame-
88 ters are varied (section 2a), and use of clustering algorithms for identifying objects in the
89 forecast field (section 2b). The object features examined here, generally of interest in many
90 applications, include size, location, intensity, and shape, all of which can be readily estimated
91 from the forecasts directly (section 2c). Section 2d describes multivariate multiple regres-
92 sion for assessing the impact of the model parameters on the distribution (across the forecast
93 domain) of object features. Anticipating the problems associated with multiple hypothesis
94 testing, steps are taken to first reduce the number of tests, and then to control different error
95 rates (section 2e). Ultimately boxplots and confidence intervals are used to visually display
96 the daily variability of the sensitivities. Section 2f summarizes all of these components, and
97 is followed by a demonstration of the methodology on forecasts from a weather prediction
98 model (section 3). The paper ends with a statement of the conclusions, additional discussion,
99 and ways in which the methodology can be generalized (section 4).

100 **2. Method**

101 *a. Data*

102 The numerical model employed to demonstrate the methodology is COAMPS[®] (Hodur
103 1997), for which some SA work has already been done. Doyle et al. (2011) and Jiang and
104 Doyle (2009) examine the effect of model parameters on mountain waves. Motivated by
105 the work of Holt et al. (2011) who studied the effect of 11 model parameters on various
106 characteristics of the forecasts, Marzban et al. (2014) used a global, variance-based SA to

107 study the effect of the same parameters and their interactions on mean (across the forecast
108 domain) and the center-of-gravity of precipitation. By contrast, here, the effect of the model
109 parameters is assessed on features of objects within the forecast field. As discussed in section
110 2c, a total of six features are examined, together summarizing the location, intensity, and
111 the shape of each object.

112 These 11 parameters are the inputs to the numerical model, and the outputs are forecasts
113 of precipitation at each of 45×72 grid points, with a spacing of $81km$, covering the entire
114 continental US, including coastal regions, and portions of Canada and Mexico. The SA
115 method developed here requires data - technically, *computer data* - which are created by
116 generating an ensemble (or sample) of input values, assimilating surface observations, and
117 then running the model forward to produce 24h forecasts of precipitation amount at each grid
118 point. As such, the SA results are contingent on the nature of this data, and consequently,
119 care must be taken in the data-generation step of the methodology.

120 The data used for the SA must be representative of the range of phenomena observed
121 at large. To that end, the present application involves a wide range of weather phenomena,
122 spanning 120 days from February 16 through July 2, 2009. Confirmed by visual examination
123 of all 120 forecasts, this temporal period includes a comprehensive series of midaltitude
124 synoptic systems traveling across the northern portion of the domain. These synoptic systems
125 extend down into the southeastern US early in the period and are replaced by subtropical
126 convective systems in the late spring and summer months. This subtropical activity also
127 occurs in the southwestern portion of the domain (west coast of Mexico) during June and
128 July in association with the southwest monsoon. The only apparent atypical weather appears
129 to be a greater amount of convective activity off the east coast of the US associated with

130 quasi-stationary or slow moving frontal systems during the period.

131 It is important that the data cases are as independent as possible. To that end, the 120
132 days are sampled at 3-day intervals in order to minimize temporal dependency, leading to
133 40 days for the analysis.

134 For each of the 40 days, 99 different values for 11 parameters are generated by Latin
135 Hypercube Sampling (LHS). Said differently, for each day, a sample of size 99 is taken from
136 the 11-dimensional space of the model parameters. This so-called “space-filling” sampling
137 scheme assures that no two of the 99 points have the same value for any of the 11 parameters.
138 It can be shown that this property leads to more precise estimates (at least, no less-precise
139 estimates) than many other sampling schemes (Cioppa and Lucas 2007; Montgomery 2009;
140 Marzban 2013). LHS is appropriate when the model parameters are all continuous quantities
141 (i.e., taking values on the Real line). For discrete or categorical inputs, Latin Square Designs
142 or Fractional Factorial Designs can be employed to produce optimal samples (Montgomery
143 2009); these methods will be demonstrated in a separate article.

144 Given that daily variability is a common source of variability in models dealing with
145 Earth systems, one question that arises is whether one should use a given LHS sample for all
146 days in the analysis. Here, in order to explore a larger portion of the model parameter space,
147 the LHS sample is allowed to vary across each of the 40 days in the study. Although this
148 choice confounds variability due to model parameters with daily variability, it is arguably a
149 better choice than the alternative (of using the same LHS sample across all days) because
150 the final sensitivity results will not be contingent on a given LHS sample.

151 The 11 model parameters are shown in Table 1; the choice of these parameters is ex-
152 plained in Holt et al. (2011). As mentioned in that paper, these parameters were chosen

153 for their anticipated sensitivity (through model tests and discussions with developers) of the
154 parameterizations in an effort to choose parameters most likely to produce changes in the
155 model output precipitation fields. Also, to focus on heavy precipitation, only the grid points
156 whose convective precipitation amount exceeds the 90th percentile of precipitation across
157 the domain are analyzed.

158 *b. Cluster Analysis*

159 There exists a wide range of clustering methods, each with their respective parameters
160 (Everitt 1980). At one extreme, there exists a class of clustering methods wherein the
161 desired number of cluster, NC , is specified by the user. A proven example in this class is
162 called Gaussian Mixture Model (GMM) clustering (McLachlan and Peel 2000). At the other
163 extreme, there exist clustering routines where NC does not play a role at all. One such
164 method is called Density-Based Spatial Clustering of Applications with Noise (DBSCAN)
165 (Ester et al. 1996). DBSCAN has two parameters, here denoted ϵ and min_samples . Roughly
166 speaking, ϵ is the maximum distance between two grid points in order for them to be in the
167 same cluster, and min_samples is the minimum number of grid points necessary to form a
168 cluster.

169 Here, these two approaches are selected for demonstration because they allow for two
170 very different ways in which a user can inject *a priori* knowledge into the analysis. For
171 example, in some applications it may be more natural to specify the number of clusters, in
172 which case GMM is a natural choice. On the other hand, DBSCAN is more natural if the
173 user has knowledge of the typical size and distance between clusters. For example, consider

174 a situation wherein the grid-spacing is relatively large (as is the case in this paper, i.e.,
175 $81km$), allowing one to examine only large scale precipitation. Although time of year and
176 location are also important, if one were to focus only on winter months in, say, the Pacific
177 Northwest, then it is reasonable to set ϵ to 3 or 4. By contrast, if one is considering jet
178 streaks, e.g., where some maximum wind speed value is reached, then ϵ can be closer to 1.
179 As for `min_samples`, 4 or 5 are reasonable values for both precipitation and jet streak events,
180 at the model resolution used here.

181 In addition to the way in which the respective parameters are handled, another reason
182 why these two clustering methods are used here is that they occupy two other extremes in the
183 family of clustering algorithms: GMM clustering belongs to a class of model-based algorithms
184 (Banfield and Raftery 1993; Fraley and Raftery 2002) common in statistics circles because
185 they are conducive to performing statistical tests, while DBSCAN assumes no underlying
186 model, and for this reason is often employed in machine learning applications.

187 For the SA component of the methodology developed here, it is not necessary for the
188 objects to be defined by these or any other clustering algorithm; the objects may be defined
189 by any other criterion or even by human experts. But some general guidance on the available
190 options may be in order. As mentioned previously, some algorithms require the specification
191 of the number of clusters (e.g., GMM) while others require information on the desired size
192 and/or distance between clusters (e.g., DBSCAN). There exists another class of clustering
193 algorithms wherein no such specification is required; an example of this type is the hierar-
194 chical agglomerative clustering (Everitt 1980), wherein the procedure begins by assigning
195 each of N points to a unique cluster, and then proceeds by combining the clusters system-
196 atically until all points are members of a single cluster. As such, this algorithm allows the

197 number of clusters to vary systematically from N to 1. A variation on this routine involves
198 the reverse procedure wherein the number of clusters is varied from 1 to N . The clustering
199 results may depend on the choice of these procedures, and so, for any specific problem some
200 trial-and-error experimentation is recommended.

201 In clustering algorithms that rely on a notion of distance, there are two types of distance
202 that must be distinguished, generally referred to as intra-cluster and inter-cluster. The for-
203 mer refers to the distance between any two points, while the latter gauges the “distance”
204 or similarity between two clusters. On gridded fields, the notion of an intra-cluster dis-
205 tance is itself ambiguous; two common choices are the Euclidean distance (defined by the
206 Pythagorean theorem), and the Manhattan distance (defined by the sum of the grid lengths
207 connecting two grid points). Although the resulting clusters do depend on the choice of this
208 distance measure, the former generally lead to smaller and more distant clusters. Here, in
209 DBSCAN, the Euclidean intra-cluster distance is used; GMM does not involve the notion of
210 an intra-cluster distance.

211 In clustering algorithms that involve the notion of an inter-cluster distance, some con-
212 sideration must be given to at least three common measures: 1) the group-average distance
213 (defined as the average of the intra-cluster distances between all the points across two clus-
214 ters), 2) the distance between the closest grid points across the two clusters, and 3) the
215 distance between the farthest grid points across the clusters. The last two options are often
216 called SLINK (for Shortest or Single link), and CLINK (for Complete link), respectively.
217 Again, the final clustering results may depend on the choice of this distance, but CLINK
218 generally results in tightly packed, small clusters. By contrast, SLINK leads to long and thin
219 clusters. A comparison of these distance measures in clustering of precipitation forecasts is

220 performed in Marzban and Sandgathe (2006). GMM and DBSCAN do not employ a notion
221 of inter-cluster distance.

222 Given that all of the above-mentioned choices may affect the final clustering result, and
223 the fact that the notion of an object is user-dependent, no specific choice is recommended
224 here. A similar philosophy is adopted with respect to the values of the parameters of the
225 clustering algorithms; they may be specified by the user, or varied across a range of values,
226 depending on the specific application. Although there exist statistical criteria that lead to
227 unique values for the parameters, the criteria involve the optimization of some other quantity,
228 e.g., Akaike Information Criterion (AIC) or Bayesian Information Criterion (BIC). As such,
229 the ambiguity in the choice of the clustering algorithm, or the values of their parameters, is
230 simply replaced with the ambiguity of selecting the appropriate criterion. Therefore, again,
231 no attempt is made to optimize the values of the parameters. It is assumed that the user has
232 sufficient information about the underlying physics to either specify the number of physical
233 objects (or a range thereof), or the typical size and distance between physical objects.

234 *c. Cluster Features*

235 In spatial verification some of the errors that are of interest include displacement, in-
236 tensity, size/area, and shape error. The estimation of these errors presumes the ability to
237 compute, respectively, the location, intensity, area, and shape of a cluster. Here, the latitude
238 and longitude of the centroid of a cluster are taken as coordinates of its location; intensity is
239 measured by the median (across the spatial extent of the cluster) of precipitation; and area
240 is measured by the number of grid points in a cluster. The shape of a cluster in GMM is

241 an ellipse because that is the cross-section (i.e., level-set) of a bivariate Gaussian. Then, the
242 eccentricity and orientation of the semi-major axis of the ellipse are natural for quantifying
243 the shape of clusters. In DBSCAN, clusters are not restricted to have any specific shape. In
244 order to be able to compare the two clustering algorithms, here an elliptical shape is assumed
245 for the clusters, and the eccentricity and orientation are obtained from the first and second
246 eigenvectors of the covariance matrix computed from the coordinates of all the grid points in
247 a given cluster. The length of the semi-major axis is set to the largest eigenvalue. The ability
248 to estimate the shape of the ellipse from the covariance matrix is an important component
249 of the methodology, because the alternative of fitting curves through the edges of clusters
250 is a much more complicated task. This covariance matrix is central to the construction of
251 many other features of potential interest (Bookstein 1991).

252 In short, the six cluster features examined here are latitude, longitude, intensity, area,
253 orientation, and eccentricity. It is worth reiterating that these quantities can be estimated
254 from the forecast field, directly, without any further modelling of the objects. Also, as
255 explained in the next section, in order to assess how the distribution (across the forecast
256 field) of a given feature is affected by the the model parameters, the former is summarized
257 with three moments - minimum, median, and maximum.

258 *d. Statistical Model*

259 The SA methodology in Marzban et al. (2014) is a variance-based approach which allows
260 one to identify linear or nonlinear relationships between the forecast quantities and the model
261 parameters, and even interactions between the model parameters. As a first approximation,

262 however, it is sufficient to estimate only the linear (i.e., main) effects, because nonlinear and
263 interaction effects are often much smaller than main effects; see, for example, pages 192, 230,
264 272, 314, 329 in Montgomery (2009), and pages 33-34 in Li et al. (2006). For this reason a
265 linear regression-based model is adequate. Specifically, the effect of the model parameters is
266 assessed via the least-squares estimate of the regression coefficients β_i in

$$y = \alpha + \beta_1 x_1 + \beta_2 x_2 + \cdots + \beta_{11} x_{11} + \delta \quad , \quad (1)$$

267 where x_i denote standardized model parameters, y is some cluster feature, and δ represents
268 any source of variability in y other than from the model parameters. This linear model is
269 further justified by the results (shown below) because when it is specialized to the case of
270 one cluster (i.e., the entire spatial domain), it reproduces the results of the variance-based
271 approach reported in Marzban et al. (2014).

272 There exists a realization of Eq. (1) in which the response is vector-valued; the model is
273 called Multivariate Multiple Regression (MMR), wherein Eq. (1) is understood as a vector
274 equation, where y , α , and β_i are all vectors (Fox et al. 2013; DelSole and Yang 2011; Rencher
275 and Christensen 2012). Ideally one could allow each component of the response vector to
276 represent a forecast feature of a given object. However, the number of objects/clusters varies
277 across the 99 values of the parameters and across days in the data. Methods for estimating
278 MMR coefficients when the number of responses is a random variable (varying across cases)
279 are not readily available. Therefore, for each of the six features measuring location, intensity
280 and shape, three summary measures are considered: the minimum, median, and maximum
281 (across the clusters in the domain) of the feature. These three quantities can be thought of
282 as a 3-point summary of the distribution (technically, histogram) of the feature, and they

283 serve as the three responses in MMR. In short, the statistical model used here is

$$\begin{pmatrix} y_d^{min} \\ y_d^{med} \\ y_d^{max} \end{pmatrix} = \begin{pmatrix} \alpha_d^{min} \\ \alpha_d^{med} \\ \alpha_d^{max} \end{pmatrix} + \begin{pmatrix} \beta_{1,d}^{min} \\ \beta_{1,d}^{med} \\ \beta_{1,d}^{max} \end{pmatrix} x_{1,d} + \begin{pmatrix} \beta_{2,d}^{min} \\ \beta_{2,d}^{med} \\ \beta_{2,d}^{max} \end{pmatrix} x_{2,d} + \dots + \begin{pmatrix} \beta_{11,d}^{min} \\ \beta_{11,d}^{med} \\ \beta_{11,d}^{max} \end{pmatrix} x_{11,d} + \begin{pmatrix} \delta_d^{min} \\ \delta_d^{med} \\ \delta_d^{max} \end{pmatrix} \tag{2}$$

284 where min, med, and max denote the minimum, median, and maximum (across clusters),
 285 respectively, and $d = 1, 2, \dots, 40$ days. In this equation, the index corresponding to the
 286 99 samples, across which the regression is performed, has been suppressed. As mentioned
 287 previously, the 99 samples of the 11 model parameters are allowed to vary across the 40 days
 288 - hence the d subscript on the x 's in Eq. (2).

289 In addition to serving as a 3-point summary of the distribution of features, the minimum,
 290 median, and maximum also serve another purpose; the median is useful, because one can
 291 assess the effect of the model parameters on a “typical” cluster; the minimum and maximum
 292 across clusters are useful because they allow one to assess whether a model parameter has
 293 an effect on **any** of the clusters in a field. For example, if it is found that a particular model
 294 parameter is positively (negatively) associated with the minimum (maximum) size across
 295 clusters, then one can conclude that the size of at least one of the clusters in the field is
 296 affected by that parameter. This is an important consideration, because if the size of at least
 297 one of the clusters is not affected by a parameter, then that parameter can be said to have
 298 no effect on the size of clusters.

299 One may wonder why it is important to use MMR with three responses, as opposed to
 300 three single-response multiple regression models; it is easy to show that the latter ignores
 301 the correlation between the response variables (Fox et al. 2013; Rencher and Christensen

302 2012). As such, MMR provides a better model of the underlying relationship between the
303 model parameters and the response variables.

304 The data on the response variables y are log-transformed to assure more bell-shaped
305 histograms; this transformation is not necessary, but is useful when the regression coefficients
306 are subjected to statistical tests, because many such tests assume relatively bell-shaped
307 distributions.

308 *e. Significance Tests*

309 Testing the coefficients in the MMR model involves performing a large number of statis-
310 tical tests ($40 \times 11 \times 6 \times 3$): one on each of 40 days, for each of 11 parameters, for each of six
311 cluster features, and for each of three summary measures across clusters. A large number
312 of tests, in turn, leads to an exponential growth in the probability of making some Type I
313 error. In general, the increase in the probability of making errors associated with multiple
314 tests is known as the multiple hypothesis testing problem (Benjamini and Hochberg 1995;
315 Bretz et al. 2001; Dmitrienko et al. 2009; Montgomery 2009; Rosenblatt 2013; Wilks 2011).

316 There exist several procedures for addressing this problem, and they all involve two
317 ingredients: 1) A set of “raw” p-values resulting from multiple hypothesis tests, and 2) the
318 specification of an error rate to be controlled. Then, the p-values are corrected (usually
319 scaled) in order to control the error rate. Two common measures of error rate are the
320 Family-wise Error Rate (FWER), defined as the probability of at least one Type I error, and
321 the False Discovery Rate (FDR), which is the expected proportion of Type I errors among
322 all the tests that lead to the rejection of the null hypothesis. One of the simplest procedures

323 for correcting the p-values involves simply multiplying all of the p-values by the number
324 of tests, and then comparing these corrected p-values with a fixed significance level (e.g.
325 0.05). This correction controls the FWER, and is called the Bonferroni correction (Bretz
326 et al. 2001; Wilks 2011). One of the popular procedures for controlling the FDR, due to
327 Benjamini and Hochberg (1995), similarly involves scaling each p-value but by a quantity
328 that depends on the rank of the p-value. The choice of the error rate to be controlled is
329 sometimes evident from the nature of the problem (Rosenblatt 2013), but not in the present
330 case; for this reason, both corrections are examined.

331 Quite independently of the above methods for controlling the errors arising from the
332 multiplicity of tests, there exists a procedure which is often practiced when one is faced
333 with multiple hypothesis tests. The main goal of the procedure is to reduce the number
334 of tests performed, and it is generally possible to do so in tests that involve linear models
335 (Montgomery 2009). In the first stage of the procedure, one performs a single, often-called
336 omnibus, hypothesis test of whether **any** of the predictors (here, model parameters) in
337 the linear model have an effect on **any** of the responses. If the null hypothesis cannot be
338 rejected, then no more tests are performed, and the conclusion of the analysis is that there is
339 no evidence that any of the parameters have an effect on any of the responses. If, however,
340 the null hypothesis is rejected, then, and only then, one proceeds to the second stage of
341 testing the significance of each of the parameters, separately.

342 In the present application, the omnibus test used in the first stage is called the Pillai's
343 trace test (Fox et al. 2013; Rencher and Christensen 2012), and its use reduces the total num-
344 ber of tests from $(40 \times 11 \times 6 \times 3)$ to only 40×6 . Here, both FWER- and FDR-controlling
345 corrections to these p-values are examined. The second stage of the aforementioned pro-

346 cedure calls for testing the effect of each of the model parameters separately, but only for
347 those comparisons that have been found significant in the first stage. However, here, for the
348 this second stage, no hypothesis testing is performed at all, because in spite of the plethora
349 of p-values they provide no information on the **magnitude** of the effect of each parameter.
350 Instead, in the second stage, we examine the boxplot of the estimated regression coefficients
351 as well as the associated confidence intervals.

352 The boxplots are generated and interpreted as follows. For each of the six cluster features,
353 for each of the three summary measures (minimum, median, and maximum across clusters
354 in the whole field), boxplots of the regression coefficients for the 11 model parameters are
355 produced. The degree of overlap between each boxplot and the number zero reflects a visual
356 (though qualitative) assessment of both the statistical significance and the magnitude of the
357 effect of the corresponding model parameter on the response: If zero is well within the span
358 of the boxplot, then one cannot conclude anything regarding the effect; if the boxplot is
359 significantly above (below) zero, then one can conclude that the corresponding parameter
360 has a positive (negative) effect on the response in question; and in such a case, the “distance”
361 of the boxplot relative to zero provides a visual indication of the magnitude of the effect.

362 The confidence interval for the mean (across 40 days) of the regression coefficient is
363 computed from the estimates of the daily regression coefficients and their standard errors,
364 all computed within MMR. Given that each of the aforementioned displays in the final
365 “output” of the methodology involves 11 CIs, a Bonferroni correction is introduced in order
366 to assure that FWER is maintained at 5%. The interpretation of the CIs is similar to that
367 of the boxplots. If a CI excludes the number zero, one can reject the null hypothesis of no
368 effect with (at least) 95% confidence; otherwise, there is no evidence to draw any conclusion.

369 The overall position of the CI conveys information on the magnitude of the effect.

370 A brief discussion of the advantages and disadvantages of the boxplot and the Confidence
371 Interval (CI) is in order. The boxplot can be considered to provide a 5-point summary of
372 the empirical sampling distribution of a regression coefficient. The sampling distribution is
373 more fundamental than the CI (and the p-value) in the sense that the latter is derived from
374 the former, and as such, the sampling distribution contains more information. However, this
375 additional information comes at the cost of less rigor, for hypothesis testing with boxplots
376 is inherently qualitative. CIs introduce a more rigorous display, but they too have some
377 limitations. For example, whereas hypothesis testing with boxplots does not require a notion
378 of a confidence level, CIs depend explicitly on that notion. Furthermore analysis of multiple
379 CIs suffers from the same problems that arise in multiple hypothesis testing with p-values
380 (see section 2e). Another limitation of CIs is that they are generally symmetric, and so, do
381 not convey information on the shape (e.g., skew) of the underlying distribution - boxplots
382 do; see the discussion section for other alternatives. Given the different trade-offs between
383 boxplots and CIs, both are used here. Consequently, the final output of the methodology
384 will consist of a figure involving 11 boxplots and CIs (one per model parameter), for each of
385 six forecast features, and three summary measures (minimum, median, maximum) thereof.

386 *f. Summary of Method*

387 This subsection summarizes the main ingredients of the proposed methodology and the
388 associated problems (and solutions) that arise in an object-based SA. See the flowchart in
389 Fig. 1.

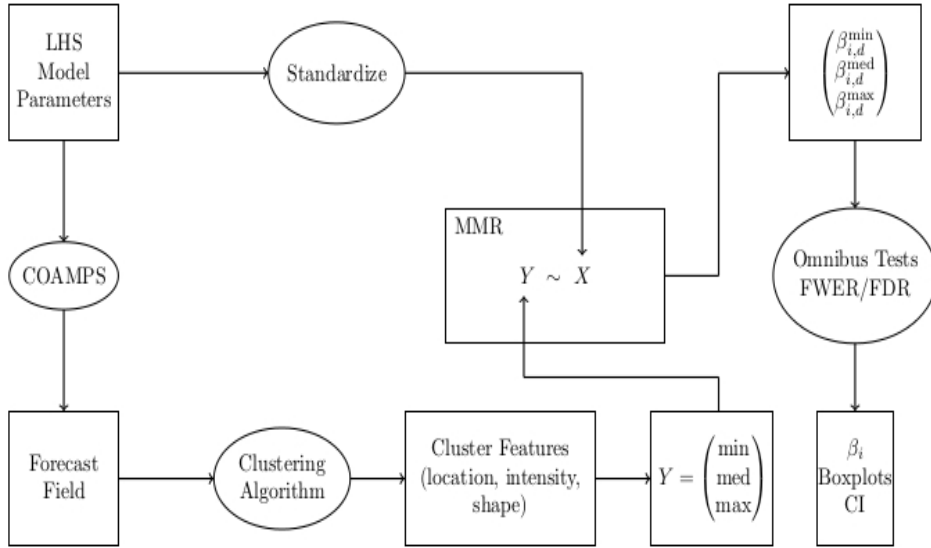


FIG. 1. The flowchart highlighting the main components of the methodology.

390 In SA, when the model parameters are continuous, a common method for varying them
 391 is LHS. It is important to point out that in models wherein daily variability is present, it is
 392 advisable to allow the LHS to vary across days.

393 The model, here COAMPS, is then run for each of the model parameter values in the
 394 LHS, and each of the generated forecast fields is subjected to cluster analysis for the purpose
 395 of identifying objects in the forecast fields. The choice of the clustering algorithm is an
 396 important consideration. Some users may wish to use algorithms in which the number of
 397 objects is specified, while other may find it more natural to specify the typical size and/or
 398 distance between objects. GMM and DBSCAN are examples from each category. Yet other
 399 users may wish to examine all possible clusterings of a field, in which case a hierarchical
 400 method is more advisable.

401 After the objects have been identified, one must decide what object features are of
 402 interest. Features that can be estimated directly from the forecast field, without further

403 modelling, are desirable. The six features proposed here are all readily computed from the
404 forecast field and its spatial covariance matrix.

405 Given the variability of the object features across the forecast domain, it is then im-
406 portant to assess the effect of the model parameters on the distribution of object features,
407 because the model parameters affect the various objects within a forecast field in differ-
408 ent ways. As such, assessing the effect of model parameters on the distribution of features
409 presents a more complete picture of sensitivities than point estimates. Here, a 3-point sum-
410 mary of the distribution is considered: the minimum, median, and maximum.

411 The question then arises as to how to model the effect of the model parameters on
412 that distribution. Here, it is shown that MMR, with multiple responses corresponding to
413 different moments of the distribution of a features, constitutes an elegant solution. Most
414 notably, MMR allows for omnibus tests of statistical significance which dramatically reduce
415 the number of hypothesis tests. Other steps are also taken to control the error rate associated
416 with multiple hypothesis testing. Then, for each day ($d = 1, \dots, 40$), the MMR coefficients
417 $\beta_{i,d}^{min}, \beta_{i,d}^{med}, \beta_{i,d}^{max}$, with $i = 1, \dots, 11$, provide estimates of the impact of the i^{th} parameter on
418 the distribution of cluster features.

419 Finally, given the importance of assessing daily variability (at least in the present ap-
420 plication), it is proposed that displaying the boxplot of the sensitivities (i.e., the β 's) across
421 days is more useful than reporting p-values. Such boxplots, although more qualitative than
422 p-values, are more effective in visually displaying both the magnitude and the variability
423 of the sensitivities. Additionally, CIs are also displayed for the purpose of rendering the
424 analysis somewhat less qualitative; see the discussion section for further alternatives.

3. Results

As mentioned previously, 24h forecasts are produced for 40 days, each with 99 different values of 11 parameters in COAMPS. Each forecast field is clustered, and three summary measures (minimum, median, and maximum, all across clusters) are computed, each for six cluster features (latitude, longitude, intensity, area, orientation, and eccentricity). First, an omnibus test is performed to test whether any of the 11 parameters have an effect on any of the three summary measures, on each day and for each cluster feature. Then, six MMR models are set up mapping the 11 parameters to three response variables. The daily variability - displayed as boxplots and confidence intervals - for each of the regression coefficients offers a visual assessment of both the statistical significance and the magnitude of the effect of each parameter.¹

The possibility of performing omnibus tests in MMR reduces the number of tests from $(40 \times 11 \times 6 \times 3)$ to $(40 \times 6) = 240$. The individual p-values are not shown here, but for DBSCAN their histogram is shown in Fig. 2. Evidently, all of the comparisons yield extremely small p-values. At a significance level of 0.05, out of the 240 tests, 53 p-values are not significant when using DBSCAN and 67 are not significant when using GMM. To emphasize the importance of this result, consider the hypothetical situation in which all of these p-values were found to be not significant. In that case, no further hypothesis testing would be necessary at all. Indeed, an examination of the individual p-values displayed in Fig. 2, reveals that a vast majority of the non-significant results are associated with the tests

¹Detailed results on clustering are available; they are suppressed here only to focus on the object-based SA methodology as a whole.

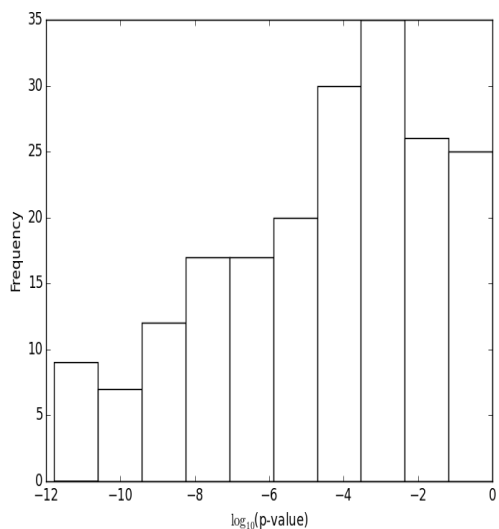


FIG. 2. Histogram of p-values from the omnibus tests across all days and response variables.

445 when the feature is the eccentricity of an object. As such, one may anticipate that none
 446 of the parameters have any effect on eccentricity. The smallness of the remaining p-values,
 447 however, calls for proceeding to the second stage of analysis.

448 The Bonferroni correction for controlling the FWER requires multiplying all of the p-
 449 values by the number of tests (i.e., 240). This correction leads to many more nonsignificant
 450 comparisons: 129 for DBSCAN and 111 for GMM. Upon making this correction, in addition
 451 to eccentricity some of the other features also emerge as being unaffected by any of the
 452 11 parameters. Further details of these results are presented below. When the Benjamini
 453 and Hochberg (1995) procedure is applied to control FDR, the number of nonsignificant
 454 comparisons is similar to those from the uncorrected tests, i.e., 60 for DBSAN and 74 for
 455 GMM.

456 As mentioned previously, although these rigorous considerations based on p-values are
 457 important to assure that the number of false alarms is tamed, it is equally useful to examine

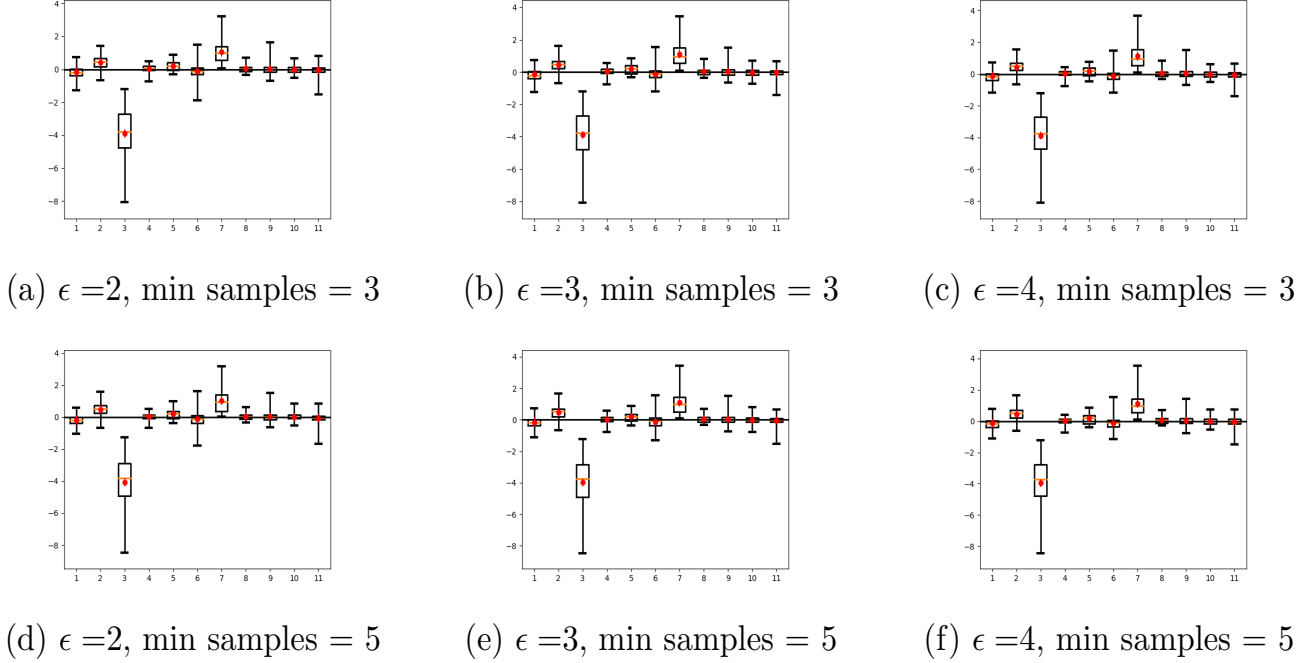


FIG. 3. Estimated regression coefficients (i.e. sensitivity of the model parameters) with median precipitation of the clusters as the response, after clustering with DBSCAN with various parameter values. The red symbols are 95% simultaneous CIs.

458 the boxplot summary of the empirical sampling distribution and CIs of the effects. Figure 3
 459 shows the sensitivity results when the response is the median (across clusters) of precipitation
 460 intensity, and DBSCAN is employed with different parameters. The analogous results for
 461 GMM with different values of NC are not shown here, but they are similar. Recall that the
 462 variability displayed in each boxplot is due to the 40 days examined. First, note that all of
 463 the panels are mostly similar to one another, which implies that the sensitivity results are
 464 mostly unaffected by the parameters of the clustering algorithm.

465 It can also be seen that many of the 11 parameters have a boxplot of values mostly
 466 around zero. In other words, when considered across multiple days most of the 11 model
 467 parameters have no effect on the median of precipitation, The most obvious exception is

468 parameter 3, which by virtue of having mostly negative values for its regression coefficient,
469 is negatively associated with median precipitation. Parameter 7 not only has a weaker
470 effect (because the median of the corresponding boxplot is closer to zero), it is also not
471 as statistically significant (because zero falls well within the span of the boxplot). This
472 parameter is positively associated with precipitation intensity in the typical (median) cluster,
473 i.e., increasing the parameter leads to more intense clusters; more, below. The conclusions
474 drawn from an analysis of the CIs in Fig. 3 are the same.

475 All of these findings are consistent with those found for convective precipitation in
476 Marzban et al. (2014) where a variance-based sensitivity was performed without any clus-
477 tering at all. This consistency adds justification to the local/regression-based SA adopted
478 here, i.e., Eq. (2). It is important to point out that this consistency does not imply that
479 an object-based SA offers nothing more than traditional non-object-based SA; the former
480 assesses the sensitivity of object features, something that cannot be done in the latter.

481 Figure 4 shows the effect of the model parameters on the latitude and longitude of the
482 clusters (top two rows), amount of precipitation (middle row) in the clusters, and the area
483 and orientation of the clusters (bottom two rows). The three columns correspond to the
484 minimum, median, and maximum of a feature. Eccentricity has also been examined, but
485 the results are not shown here because it is not affected by any of the 11 parameters; this
486 conclusion is consistent with the results of the omnibus tests performed in the first stage,
487 mentioned above.

488 Examination of all of the panels suggests that parameters 4, 5, 8, 9, 10, 11 have little or
489 no effect on any of the object features. By contrast, parameters 1, 2, 3, 6, and 7 appear to
490 have varying effects depending on the object feature. Also, the orientation (in addition to

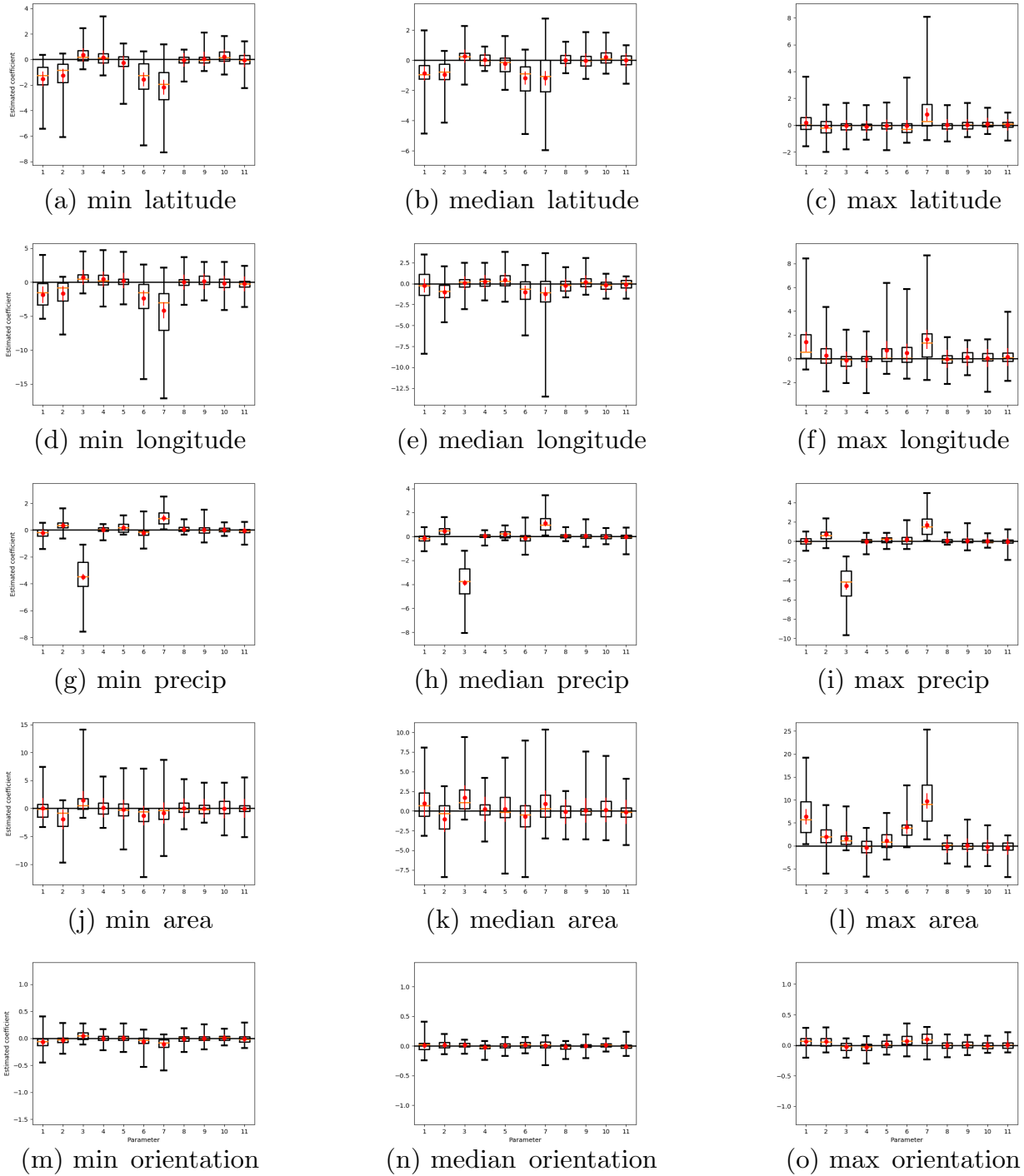


FIG. 4. Estimated MMR coefficients (i.e. sensitivity of the model parameters) on three summary measures (minimum, median, maximum) of different cluster features (latitude, longitude, amount of precipitation, and area and orientation of clusters. Eccentricity is not shown (see text). The red symbols are 95% simultaneous CIs. The clustering is done with DBSCAN with $\epsilon = 2\sqrt{2}$, `min_samples` = 3.

491 eccentricity) of the clusters is unaffected by any of the parameters.

492 The strongest effects are from parameters 3 and 7 on the amount of precipitation. This
493 relationship was already examined in Fig. 3; but now the same pattern can be seen in the
494 minimum, median, and maximum intensity (panels g, h, i in Fig. 4), which implies that the
495 effect of parameters 3 and 7 is to shift down and up, respectively, the whole distribution of
496 precipitation intensity.

497 The next strongest effects are those of parameters 1 and 7 on maximum area (panel l).
498 Given that these two parameters have no effect on the minimum and median area (panels j
499 and k), it follows that these parameters affect only the right tail of the distribution of size. In
500 other words, by contrast to precipitation intensity whose distribution shifts when parameter
501 7 is varied, the distribution of size is stretched when that parameter changes. Parameter 6,
502 too, appears to have an effect on maximum area, but to a lesser extent, both statistically
503 and in magnitude.

504 Whereas parameter 1 tends to stretch out the distribution of area to the right, it appears
505 to have the opposite effect on the minimum and median longitude of the clusters. The effect
506 is weak in magnitude, but statistically significant. It does not affect the maximum longitude
507 (panel f), and so, it stretches the distribution of longitude on the left, causing clusters to
508 appear with smaller longitude, which given the encoding of the data used here, means to the
509 west. Parameters 2, 6, and 7 appear to have the same effect as parameter 1.

510 The latitude appears to be weakly affected by some of the parameters. For example,
511 parameter 7, and to a much lesser degree parameter 1, is positively associated with median
512 and maximum latitude, but negatively associated with minimum latitude. In other words,
513 increasing parameter 7 increases the width of the distribution of latitude values, causing

514 them to be more spread out along the latitudes.

515 All of the above conclusions are based on clustering with DBSCAN with $\epsilon = 2\sqrt{2}$ and
516 `min_samples=3`. To test the robustness of these results the same analysis was repeated but
517 with GMM as the clustering algorithm and with $NC = 3$. The results (not shown here) are
518 mostly the same. One relatively clear difference between the DBSCAN and GMM results is
519 in the effect of parameters 1 and 7 on area; whereas with DBSCAN those parameters have
520 an effect only on the maximum area, the results based on GMM suggest a significant effect
521 on all three distribution summary measures (minimum, median, and maximum area).

522 Further differences between DBSCAN and GMM sensitivity results are found when one
523 performs a multivariate test for the effect of the model parameters across **all** days. For
524 DBSCAN, the p-values corresponding to each of the six cluster features are all found to be
525 nearly zero. So, some of the model parameters do have a significant effect on some of the
526 features. The same is true for GMM, with the exception of latitude and eccentricity for which
527 there is no evidence of an effect (p-values 0.435 and 0.290, respectively). It may appear that
528 these results are contradictory, but they are not because the respective parameters of the
529 two clustering algorithms have not been tuned to render them comparable. Specifically, the
530 DBSCAN parameters are $\epsilon = 2\sqrt{2}$ and `min_samples=3`, while for GMM the parameter NC
531 is set to three. In other words, the differences are due to the way in which the two clustering
532 algorithms handle their respective parameters. As mentioned earlier, such differences do not
533 point to defects in the methodology; they simply reflect the choice of what the user considers
534 to be an object.

535 4. Conclusion and Discussion

536 It is shown that by employing methods of cluster analysis and sensitivity analysis one
537 can assess the magnitude and statistical significance of the effect of model parameters on
538 the distribution of features (location, intensity, size, and shape) of objects within forecast
539 fields. For example, one can reveal the model parameters that affect the overall location
540 and/or width of the distribution of object features, and those which impact the shape of the
541 distribution, e.g., by stretching out the left and/or right tail. The approach does not point to
542 any “optimal” values of the model parameters, for that would require optimizing the model
543 parameters to maximize some measure of agreement between forecasts and observations. In
544 other words, although the work here lays the foundation for tuning the model parameters
545 for the purpose of improving forecasts in terms of metrics that arise naturally in spatial
546 verification/evaluation methods, no such tuning is performed here.

547 It is worth pointing out that at least in meteorology, it is not uncommon for different
548 human experts to have different notions of an object in the forecast field. As such, the
549 ambiguities discussed above are not specific to clustering algorithms, but are inherent to
550 any object-based approach. In spite of this inherent ambiguity, many spatial verification
551 techniques generally rely on some notion of an object. The main reason is that accounting
552 for objects in a forecast field is a first step in the verification/evaluation process, and the
553 manner in which objects are defined is of secondary importance.

554 While this paper is primarily about a methodology, it is worthwhile to provide a possible
555 physical explanation for at least the strongest results in the COAMPS application. The
556 strongest influence or sensitivity is from parameter 3, the fraction of available precipitation

557 fed back to the grid from the Kain-Fritsch scheme. Increasing this fraction reduces con-
558 vective precipitation and, based on the results in Marzban et al. (2014), increases stable
559 precipitation, while not affecting total precipitation. It also is responsible for weakening
560 the convective precipitation, i.e., increasing the number of weak systems. The next largest
561 sensitivity is from parameter 7, which controls the temperature difference required to ini-
562 tiate convective precipitation. Again, as shown in Marzban et al. (2014), this parameter
563 also controls a trade-off between convective and stable precipitation and has little effect on
564 total precipitation (along with parameter 1). Parameters 1 and 7 do increase the area of
565 convective precipitation in large precipitation events but not in smaller (areal) precipitation
566 events, likely due to the trade-off between stable and convective precipitation in large events
567 such as frontal systems and mesoscale clusters. This process may also explain the apparent
568 increase in east-west areal coverage and the intensification of precipitation events, as found
569 here.

570 Several generalizations of the proposed methodology are possible. In Marzban et al.
571 (2008) it has been shown that clustering can be done not only in the 2-dimensional space of
572 latitude and longitude of each grid point, but also in the 3-dimensional space that includes
573 the amount of precipitation at each grid point. In fact, one may argue that the inclusion
574 of more meteorological quantities in the clustering phase ought to lead to more meteorolog-
575 ically relevant objects being identified. In turn, this is more likely to lead to more realistic
576 representation of the effect of the parameters on the object features. The object features
577 may also be extended or revised. For example, here the shape of an object is approximated
578 by an ellipse. But it is possible to use more sophisticated methods of shape analysis (Book-
579 stein 1991; Lack et al. 2010; Micheas et al. 2007; Lakshmanan et al. 2009) to model more

580 complex shapes. Another possible generalization is to allow for interactions between model
581 parameters. Although the statistical model used here does account for covariance between
582 the model parameters, and between the response variables, no explicit interaction is intro-
583 duced. The inclusion of such terms is straightforward, and is unlikely to lead to overfitting,
584 at least in linear models such as MMR.

585 The use of boxplots (in the second stage) to visually display the daily variability of the
586 results is necessarily qualitative. But the authors believe that the information provided in
587 the visual display compensates for the lack of rigor accompanying p-values. CIs are more
588 rigorous than the boxplots, but as mentioned previously, that rigor is accompanied by loss
589 of some information. However, if even more rigor is called for, then it is possible to revise
590 the displays accordingly. For example, one option would be to include a Day factor in
591 the MMR model, and then test the model parameters. Although, the daily variability of
592 the β coefficients will be lost, each model parameter will be accompanied by a p-value.
593 Alternatively, one may compute a Bayesian intervals (Leonard and Hsu 1999); such intervals
594 are not necessarily symmetric, and therefore, will be able to convey information on the shape
595 of the underlying sampling distribution. However, they do require additional information,
596 e.g., some knowledge of the prior distribution of the β 's. All of these options will render the
597 analysis more quantitative, although with a different focus than that emphasized here.²

²The authors acknowledge an anonymous reviewer for these alternatives.

598 **5. Code and/or data availability**

599 The code and the data analyzed here occupy about 4.0G of computer space, and are avail-
600 able upon request from the corresponding author, or from <https://doi.org/10.5281/zenodo.1043542>

601 **6. Competing Interests**

602 The authors declare that they have no conflict of interest

603 **7. Acknowledgments**

604 This work has received support from Office of Naval Research (N00014-12-G-0078 task
605 29) and National Science Foundation (AGS-1402895). The authors are grateful to James
606 D. Doyle and Nicholas C. Lederer for providing invaluable support. Ethan P. Marzban is
607 acknowledged for making the flowchart in Figure 1.

608

609

REFERENCES

610 Ahijevych, D., Gilleland, D. E., Brown, B. G., and Ebert, E. E.: Application of spatial veri-
611 fication methods to idealized and NWP-gridded precipitation forecasts, *Wea. Forecasting*,
612 24, 1485–1497, 2009.

613 Backman, J., Wood, C., Auvinen, M., Kangas, L., Hannuniemi, H., Karppien, A., and
614 Kukkonen, J.: Sensitivity analysis of the meteorological pre-processor MPP-FMI 3.0 using
615 algorithmic differentiation, *Geosci. Model Dev. Discuss.*, (in review), 2017.

616 Baldwin, M. E., Lakshmivarahan, S., and Kain, J. S.: Verification of mesoscale features in
617 NWP models, in: *Amer Meteor. Soc., 9th Conf. on Mesoscale Processes*, pp. 255–258, Ft.
618 Lauderdale, FL., 2001.

619 Baldwin, M. E., Lakshmivarahan, S., and Kain, J. S.: Development of an “events-oriented”
620 approach to forecast verification, in: *15th Conf. Numerical Weather Prediction*, San An-
621 tonio, TX, 2002.

622 Banfield, J. D. and Raftery, A. E.: Model-based Gaussian and non-Gaussian clustering,
623 *Biometrics*, 49, 803–821, 1993.

624 Benjamini, Y. and Hochberg, Y.: Controlling the false discovery rate: a practical and pow-
625 erful approach to multiple testing, *J. R. Stat. Soc., B* 57, 289–300, 1995.

626 Bolado-Lavin, R. and Badea, A. C.: Review of sensitivity analysis methods and experience
627 for geological disposal of radioactive waste and spent nuclear fuel, *JRC Scientific and*
628 *Technical Report*, Available online, 2008.

629 Bookstein, F. L.: *Morphometric Tools for Landmark Data: Geometry and Biology*, Cam-
630 bridge, 1991.

631 Bretz, F., Hothorn, T., and Westfall, P.: *Multiple Comparisons Using R*, Chapman and Hall,
632 2001.

633 Brown, B. G., Mahoney, J. L., Davis, C. A., Bullock, R., and Mueller, C.: Improved ap-
634 proaches for measuring the quality of convective weather forecasts, in: 16th Conference
635 on Probability and Statistics in the Atmospheric Sciences, pp. 20–25, Orlando, FL, 2002.

636 Casati, B., Ross, G., and Stephenson, D.: A new intensity-scale approach for the verification
637 of spatial precipitation forecasts, *Met. App.*, 11, 141–154, 2004.

638 Cioppa, T. and Lucas, T.: Efficient nearly orthogonal and space-filling latin hypercubes,
639 *Technometrics*, 49(1), 45–55, 2007.

640 Davis, C., Brown, B., and Bullock, R.: Object-based verification of precipitation forecasts.
641 Part I: Methodology and application to mesoscale rain areas, *Mon. Wea. Rev.*, 134, 1772–
642 1784, 2006a.

643 Davis, C. A., Brown, B., and Bullock, R.: Object-based verification of precipitation forecasts.
644 Part II: Application to convective rain systems, *Mon. Wea. Rev.*, 134, 1785–1795, 2006b.

645 DelSole, T. and Yang, X.: Field Significance of Regression Patterns, *J. Climate*, 24, 5094–
646 5107, 2011.

647 Dmitrienko, A. A., Tamhane, C., and (ed.), F. B.: *Multiple Testing Problems in Pharma-*
648 *ceutical Statistics*, Chapman and Hall, 2009.

649 Doyle, J. D., Jiang, Q., Smith, R. B., and Grubii, V.: Three-dimensional characteristics of
650 stratospheric mountain waves during T-REX, *Mon. Wea. Rev.*, 139, 3–23, 2011.

651 Du, J. and Mullen, S. L.: Removal of Distortion Error from an Ensemble Forecast, *Mon.*
652 *Wea. Rev.*, 128, 3347–3351, 2000.

- 653 Ebert, E.: Fuzzy verification of high-resolution gridded forecasts: a review and proposed
654 framework, *Meteor. Appl.*, 15 (1), 51–64, 2008.
- 655 Ebert, E. E. and McBride, J. L.: Verification of precipitation in weather systems: determi-
656 nation of systematic errors, *Jour. Hydrology*, 239, 179–202, 2000.
- 657 Errico, R. M.: What is an Adjoint Model?, *Bull. Amer. Meteor. Soc.*, 78, 2577–2591, 1997.
- 658 Ester, M., Kriegel, H.-P., Sander, J., and Xu, X.: A density-based algorithm for discovering
659 clusters in large spatial databases with noise, in: *Proceedings of Knowledge Discovery and
660 Data Mining (KDD-96)*, vol. 96(34), pp. 226–231, 1996.
- 661 Everitt, B. S.: *Cluster Analysis*, Heinemann Educational Books, London, 1980.
- 662 Fox, J., Friendly, M., and Weisberg, S.: Hypothesis tests for multivariate linear models using
663 the car package, *The R Journal*, 5(1), 39–52, 2013.
- 664 Fraley, C. and Raftery, A.: Model-Based Clustering, Discriminant Analysis, and Density
665 Estimation, *Journal of the American Statistical Association*, 97, 611–631, 2002.
- 666 French, S., Lekic, V., and Romanowicz, B.: Waveform Tomography Reveals Channeled Flow
667 at the Base of the Oceanic Asthenosphere, *Science*, 342, 227–230, 2013.
- 668 Froyland, G., Stuart, R. M., and van Sebille, E.: How well-connected is the surface of the
669 global ocean?, *Chaos*, 24, ??, 2014.
- 670 Gilleland, D. E., Ahijevych, D., Brown, B. G., Casati, B., and Ebert, E. E.: Intercomparison
671 of Spatial Forecast Verification Methods, *Wea. Forecasting*, 24, 1416–1430, 2009.

672 Hacker, J. P., Snyder, C., Ha, S.-Y., and Pocerlich, M.: Linear and non-linear response to
673 parameter variations in a mesoscale model, *Tellus A*, 63, 429–444, doi:10.1111/j.1600-0870.
674 2010.00505.x, 2011.

675 Hodur, R. M.: The Naval Research Laboratorys Coupled Ocean/Atmosphere Mesoscale
676 Prediction System (COAMPS), *Mon. Wea. Rev.*, 125, 1414–1430, 1997.

677 Hoffman, R. N., Liu, Z., Louis, J.-F., and Grassotti, C.: Distortion representation of forecast
678 errors, *Mon. Wea. Rev.*, 123, 2758–2770, 1995.

679 Holt, T. R., Cummings, J. A., Bishop, C. H., Doyle, J. D., Hong, X., Chen, S., and Jin, Y.:
680 Development and testing of a coupled ocean-atmosphere mesoscale ensemble prediction
681 system, *Ocean Dynamics*, 61, 1937–1954, doi:10.1007/s10236-011-0449-9, 2011.

682 Jiang, Q. and Doyle, J. D.: The impact of moisture on Mountain Waves, *Mon. Wea. Rev.*,
683 137, 3888–3906, 2009.

684 Kalra, T. S., Aretxabaleta, A., Seshadri, P., Ganju, N. K., and Beudin, A.: Sensitivity
685 Analysis of a Coupled Hydrodynamic-Vegetation Model Using the Effectively Subsampled
686 Quadratures Method, *Geosci. Model Dev. Discuss.*, (in review), 2017.

687 Keil, C. and Craig, G. C.: A displacement-based error measure applied in a Regional En-
688 semble Forecasting System, *Mon. Wea. Rev.*, 135(9), 3248–3259, 2007.

689 Lack, S. A., Limpert, G. L., and Fox, N. I.: An object-oriented multiscale verification scheme,
690 *Wea. Forecasting*, 25(1), 79–92, 2010.

691 Laine, M., Solonen, A., Haario, H., and Järvinen, H.: Ensemble prediction and parameter
692 estimation system: the method, *Q. J. R. Meteorol. Soc.*, 138, 289–297, 2012.

693 Lakshmanan, V. and Kain, J. S.: A Gaussian Mixture Model Approach to Forecast Verifi-
694 cation, *Wea. Forecasting*, 25(3), 908–920, 2010.

695 Lakshmanan, V., Hondl, K., and Rabin, R.: An Efficient, general-purpose technique for
696 identifying storm cells in geospatial image, *J. Atmos. Oceanic Technol.*, 26, 523–537, 2009.

697 Leonard, T. and Hsu, J. S. J.: *Bayesian Methods; An Analysis for Statisticians and Inter-*
698 *disciplinary Researchers*, Cambridge University Press, Cambridge, 1999.

699 Li, J., Hsu, K., AghaKouchak, A., and Sorooshian, S.: An object-based approach for verifi-
700 cation of precipitation estimation, *International Journal of Remote Sensing*, 36:2, 513–529,
701 2015.

702 Li, X., Sudarsanam, N., and Frey, D. D.: Regularities in data from factorial experiments,
703 *Complexity*, 11(5), 32–45, 2006.

704 Lorenz, E. N.: Deterministic non-periodic flow, *J. Atmos. Sci.*, 20, 130–141, 1963.

705 Lucas, D. D., Klein, R., Tannahill, J., Ivanova, D., Brandon, S., Domyancic, D., and Zhang,
706 Y.: Failure analysis of parameter-induced simulation crashes in climate models, *Geosci.*
707 *Model Dev.*, 6, 1157–1171, 2013.

708 Marzban, C.: Variance-based Sensitivity Analysis: An illustration on the Lorenz '63 model,
709 *Mon. Wea. Rev.*, 141(11), 4069–4079, 2013.

710 Marzban, C. and Sandgathe, S.: Cluster analysis for verification of precipitation fields, *Wea.*
711 *Forecasting*, 21(5), 824–838, 2006.

712 Marzban, C. and Sandgathe, S.: Cluster Analysis for Object-Oriented Verification of Fields:
713 A Variation, *Mon. Wea. Rev.*, 136, 1013–1025, 2008.

714 Marzban, C., Sandgathe, S., and Lyons, H.: An Object-oriented Verification of Three NWP
715 Model Formulations via Cluster Analysis: An objective and a subjective analysis, *Mon.*
716 *Wea. Rev.*, 136 (9), 3392–3407, 2008.

717 Marzban, C., Sandgathe, S., Lyons, H., and Lederer, N.: Three Spatial Verification Tech-
718 niques: Cluster Analysis, Variogram, and Optical Flow, *Wea. Forecasting*, 24(6), 1457–
719 1471, 2009.

720 Marzban, C., Sandgathe, S., Doyle, J. D., and Lederer, N. C.: Variance-Based Sensitivity
721 Analysis: Preliminary Results in COAMPS, *Mon. Wea. Rev.*, 142, 2028–2042, 2014.

722 McLachlan, G. J. and Peel, D.: *Finite Mixture Models*, John Wiley & Sons, Hoboken, NJ
723 USA, 2000.

724 Micheas, A. C., Fox, N. I., Lack, S. A., and Wikle, C. K.: Cell identification and verification
725 of QPF ensembles using shape analysis techniques, *J. Hydrology*, 343, 105–116, 2007.

726 Montgomery, D. C.: *Design and Analysis of Experiments*, Wiley & Sons, 7th edition, 2009.

727 Nachamkin, J. E.: Mesoscale verification using meteorological composites, *Mon. Wea. Rev.*,
728 132, 941–955, 2004.

729 Ollinaho, P., ärvinen, H., Bauer, P., Laine, M., Bechtold, P., Susiluoto, J., and Haario, H.:
730 Optimization of NWP model closure parameters using total energy norm of forecast error
731 as a target, *Geosci. Model Dev.*, 7(5), 1889–1900, 2014.

732 Rencher, A. C. and Christensen, W. F.: *Methods of Multivariate Analysis*, John Wiley &
733 Sons, Inc., Hoboken, NJ, USA, doi:10.1002/9781118391686.ch10, 2012.

734 Roberts, N. M. and Lean, H. W.: Scale-Selective Verification of Rainfall Accumulations from
735 High-Resolution Forecasts of Convective Events, *Mon. Wea. Rev.*, 136, 78–97, 2008.

736 Robock, A., Luo, L., Wood, E. F., Wen, F., Mitchell, K. E., Houser, P., Schaake, J. C.,
737 Lohmann, D., Cosgrove, B., Sheffield, J., Duan, Q., Higgins, R. W., Pinker, R. T., Tarpley,
738 J. D., Basara, J. B., and Crawford, K. C.: Evaluation of the North American Land Data
739 Assimilation System over the southern Great Plains during warm seasons, *J. Geophys.*
740 *Res.*, 108, 8846–8867, 2003.

741 Roebber, P.: The role of surface heat and Moisture Fluxes Associated with large-scale ocean
742 current meanders in maritime cyclogenesis, *Mon. Wea. Rev.*, 117, 1676–1694, 1989.

743 Roebber, P. and Bosart, L.: The sensitivity of precipitation to circulation details. part i: an
744 analysis of regional analogs, *Mon. Wea. Rev.*, 126, 437–455, 1989.

745 Rosenblatt, J.: A practioner’s guide to multiple hypothesis testing error rates,
746 arXiv:1304.4920v3, 2013.

747 Safta, C., Ricciuto, D., Sargsyan, K., Debusschere, B., Najm, H., Williams, M., and Thorn-
748 ton, P.: Global sensitivity analysis, probabilistic calibration, and predictive assessment for

749 the data assimilation linked ecosystem carbon model, *Geosci. Model Dev.*, 8, 1899–1918,
750 2015.

751 Saltelli, A., Ratto, M., Andres, T., Campolongo, F., Cariboni, J., Saisana, M., and Tarantola,
752 S.: *Global Sensitivity Analysis: The Primer*, Wiley Publishing, 2008.

753 Saltelli, A., Annoni, P., Azzini, I., Campolongo, F., Ratto, M., and Tarantola, S.: Variance
754 based sensitivity analysis of model output: Design and estimator for the total sensitivity
755 index, *Computer Physics Communications*, 181, 259–270, 2010.

756 Samsel, F., Petersen, M., Abram, G., Turton, T. L., Rogers, D., and Ahrens, J.: Visual-
757 ization of Ocean Currents and Eddies in a High-Resolution Global Ocean-Climate Model,
758 in: *Proceedings of the 15th International Conference for High Performance Computing,
759 Networking, Storage and Analysis*, Austin, TX, 2015.

760 Stein, A. F., Draxler, R. R., Rolph, G. D., Stunder, B. J. B., Cohen, M. D., and Ngan, F.:
761 NOAA HYSPLIT Atmospheric Transport and Dispersion Modeling System, *Bull. Amer.
762 Meteor. Soc.*, 96, 2059–2077, 2015.

763 Venugopal, V., Basu, S., and Foufoula-Georgiou, E.: A new metric for comparing precip-
764 itation patterns with an application to ensemble forecasts, *J. Geophys. Res.*, 110, D8,
765 D08 111 10.1029/2004JD005 395, 2005.

766 Vogelmann, J. E., Kost, J. R., Tolk, B., Howard, S., Short, K., and Chen, X.: Monitoring
767 Landscape Change for LANDFIRE Using Multi-Temporal Satellite Imagery and Ancillary
768 Data, *IEEE Journal of Selected Topics in Applied Earth Observations and Remote Sensing*,
769 4(2), 252–264, 2011.

- 770 Wang, Y. H., Fan, C. R., Zhang, J., Niu, T., Zhang, S., and Jiang, J. R.: Forecast Verification
771 and Visualization based on Gaussian Mixture Model Co-estimation, *Computer Graphics*
772 *Forum*, 34, 99–110, 2015.
- 773 Wealands, S. R., Grayson, R. B., and Walker, J. P.: Quantitative comparison of spatial
774 fields for hydrological model assessment: some promising approaches, *Advances in Water*
775 *Resources*, 28, 15–32, 2005.
- 776 Wernli, H., Paulat, M., Hagen, M., and Frei, C.: SAL - A Novel Quality Measure for the
777 Verification of Quantitative Precipitation Forecasts, *Mon. Wea. Rev.*, 136, 4470–4487,
778 2008.
- 779 Wilks, D. S.: *Statistical Methods in the Atmospheric Sciences* (3rd edition), Elsevier Inc.,
780 2011.
- 781 Yu, Y. Y., Finke, P. A., Wu, H. B., and Guo, Z. T.: Sensitivity analysis and calibration of a
782 soil carbon model (SoilGen2) in two contrasting loess forest soils, *Geosci. Model Dev.*, 6,
783 29–44, 2013.

ID	Name (Unit)	Description	Default	Range
1	delt2KF ($^{\circ}C$)	Temperature increment at the LCL for KF trigger	0	-2, 2
2	cloudrad (m)	Cloud radius factor in KF	1500	500, 3000
3	prcpfrac	Fraction of available precipitation in KF, fed back to the grid scale	0.5	0, 1
4	mixlen	Linear factor that multiplies the mixing length within the PBL	1.0	0.5, 1.5
5	sfclx	Linear factor that modifies the surface fluxes	1.0	0.5, 1.5
6	wfctKF	Linear factor for the vertical velocity (grid scale) used by KF trigger	1.0	0.5, 1.5
7	delt1KF ($^{\circ}C$)	Another method to perturb the temperature at the LCL in KF	0	-2, 2
8	autocon1 ($\frac{kg}{m^3s}$)	Autoconversion factors for the microphysics	0.001	1e-4, 1e-2
9	autocon2 ($\frac{kg}{m^3s}$)	Autoconversion factors for the microphysics	4e-4	4e-5, 4e-3
10	rainsi ($\frac{1}{m}$)	Microphysics slope intercept parameter for rain	8.0e6	8.0e5, 8.0e7
11	snows_i ($\frac{1}{m}$)	Microphysics slope intercept parameter for snow	2.0e7	2.0e6, 2.0e8

KF = Kain-Fritsch, PBL = Planetary Boundary Layer, LCL = Lifted Condensation Level

TABLE 1. The 11 parameters studied in this paper. Also shown are the default values, and the range over which they are varied.